Published in AJSE, Vol:22, Issue: 1
Received on 10th December 2022
Revised on 27th February 2023
Accepted on 30th April 2023

AIUB JOURNAL OF SCIENCE AND ENGINEERING
ISSN: 1608 – 3679 (print) 2520 – 4890 (Online)

A Comparative Study of Fixing One Barrier-Varying Another Barrier for a Resonant Tunneling Diode

Tahseen Asma Meem, Shaira Tashnub Torsa., Mr. Mehedi Hasan and Mahfujur Rahman

***Abstract*— In this research paper, the effects of fixing one barrier and varying another barrier have been analyzed and compared for a GaAs/Al0.3Ga0.7As based double barrier resonant tunneling diode for two different models - Hartree Quantum Charge model and semi-classical Thomas Fermi model. VI characteristic graphs are studied to assess the overall performance of both models. The simulations are carried out in a nanoelectronics modeling tool suite – Nano electronic Modelling 5 (NEMO5) considering Non-Equilibrium Green's Function (NEGF), at room temperature of 300K and biased voltage of 0 to 0.5 V. In this paper, it was demonstrated that a very larger amount of current is supplied by both models when the first barrier is varied and second barrier is fixed in comparison to the first barrier when kept fixed and second barrier is varied. But as quantum charge inside the quantum well is existed in the Hartree model, so overall Hartree model supplied a greater amount of current compared to the Thomas Fermi model. Quantum charge inside its quantum well is not present in the Thomas Fermi model. But a better NDR region is created by the Thomas Fermi model in both varied first barrier-fixed second barrier and fixed first barrier-varied second barrier cases compared to the Hartree model. This NDR region can be used for numerous digital applications. On the other hand, a vast range of analog applications can be used by the Hartree model that produced larger current per unit voltage.**

***Index Terms*— Resonant Tunneling Diode (RTD), Double Barrier Resonant Tunneling Diode (DBRTD), Fixed Barrier, Varied Barrier, First Positive Differential Resistance (PDR1), Negative Differential Resistance (NDR), Second Positive Differential Resistance (PDR2), Non-Equilibrium Green's Function (NEGF).**

Tahseen Asma Meem is with the Department of Electrical and Electronic Engineering, American International University-Bangladesh (AIUB) at KA-66/1 old), 408/1 (new), Kuril, Kuratoli Road, Dhaka 1229, Bangladesh (e-mail: tahseen@aiub.edu).

Shaira Tashnub Torsa. is with the Department of Electrical and Electronic Engineering, American International University-Bangladesh (AIUB) at KA-66/1 old), 408/1 (new), Kuril, Kuratoli Road, Dhaka 1229, Bangladesh (e-mail: shairatashnubtorsa@gmail.com).

Mr. Mehedi Hasan is with the Department of Electrical and Electronic Engineering, American International University-Bangladesh (AIUB) at KA-66/1 old), 408/1 (new), Kuril, Kuratoli Road, Dhaka 1229, Bangladesh (e-mail: mehedi@aiub.edu).

Mahfujur Rahman was with the Department of Electrical and Electronic Engineering, American International University-Bangladesh (AIUB) at KA-66/1 old), 408/1 (new), Kuril, Kuratoli Road, Dhaka 1229, Bangladesh (e-mail: mahfuj@aiub.edu).

I. INTRODUCTION

TO represent RTD, and three equivalent proposals are worked out which include the non-equilibrium green function (NEGF) scheme, the Schrodinger equation method, and the Winger equation [1]. All the states are found with the support of open boundary conditions. At the Hartree level, the interaction of electrostatic force is taken into account. In a less particular way with Thomas-fermi approximation, the coherent property is promoted [2].

A very strongly creative and calculated model is provided by non-equilibrium green function formalism by the use of quantum transport in high-tech [3]. To add the inflexible scattering and powerful effects of correlation at an atomistic level [3], it excels in the Landauer proposition for choleric, non-interacting electrons.

The interest of using RTDs in different analog and digital applications risen gigantically after the initiating contributions of Chang, Esaki and Tsu [4]. The first presentation about the resonant tunneling structure was begun by these three researchers in 1974 [4]. They displayed RTDs as a substitute for transistors for high-frequency oscillations for use in microwave circuits and even for logic circuits. RTDs possess the widest bandwidth recently among all the semiconductor devices.

II. THEORY AND METHODOLOGY

A. *Layers of DBRTD*

There are seven different layers in a GaAs/Al0.3Ga0.7As double barrier RTD. By rising current density in RTD, contact 1 and contact 2 aid large electron count. They are also known as Lead 1 and Lead 2. By the phenomenon of highly doped contacts, spacer 1 and spacer 2 impede the diffusion of impurity atoms' scattering through two barriers and a well. In the conduction band, barrier 1 and barrier 2 operate as potential blockades for electrons. Well emerges quasi-bound states that cause resonant transmission.

Barrier 1, Barrier 2 and Well have 5 nm and they have the lowest widths. Both Spacers have 10 nm which is twice the barriers and well. Both Contacts possess 30 nm, which is the highest width. Well, Barrier 1 and Barrier 2 have widths of 25 nm less than those of Contacts, while Spacers possess 20 nm less width than Contacts.

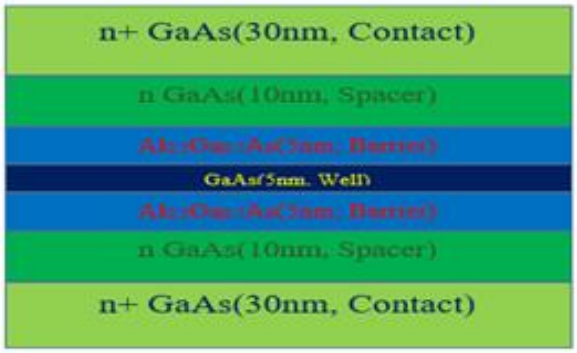

Figure 1: *Different layers of the GaAs/ Al0.3Ga0.7As based double barrier resonant tunneling diode* [5].

B. Principle of a Resonant Tunneling Diode

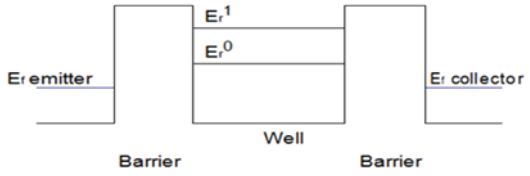

Figure 2: *Schematic Structure of DBRTD* [6].

The conduction band of a double barrier structure for various applied voltages is shown in the picture above, along with the device's consequent conduction state on the I-V characteristics. The following phenomenon happens when the collector bias is gradually increased:

Energy levels [6] (Er1 and Er0) are still above the Fermi levels when voltage is not applied (V = 0 V), and current cannot pass through the double barrier because the Fermi levels in the emitter and collector are properly aligned.

By supplying a positive voltage (V > 0), the conduction band is tilted. Energy levels in the well are pulled down and when the first resonant level reaches the Fermi level in the emitter, carriers can flow from the emitter to the collector [6]. Increasing the bias induces an increase of current until the energy level Er0 reaches the conduction band at the bottom of the emitter side. When the energy level Er0 is in front of the conduction band, the current stays at maximum.

If the collector is further biased, then the sub-band Er0 below the emitter conduction band is decreased. This turns off available electrons for tunneling through the barrier, thus the current decreases with an increased voltage that provides a negative differential resistance region (NDR).

A rise in the last bias falls the second level Er1, which enables a second tunneling process, and thermionic current is risen, which flows above the barrier [2]. In other words, the existence of a peak in the transmission coefficient is essentially what determines whether resonant tunneling current occurs across a double barrier construction. [2].

C. Equations Required for analysis of fixing one barrier-varying another barrier in a DBRTD

Five equations were used for fixed one barrier-varied another barrier analysis in a double barrier resonant tunneling diode and these five equations are:

$$PVCR = I_p/I_v \quad (1)$$

$$PVVR = V_p/V_v \quad (2)$$

$$R_n = (V_v - V_p)/ (I_p - I_V) \quad (3)$$

$$R_{p2} = (V_s - V_v)/ (I_p - I_v) \quad (4)$$

$$R_{p1} = V_p/I_p \quad (5)$$

Here,

PVCR = Peak Valley to Current Ratio
PVVR = Peak Valley to Voltage Ratio
Rn = Negative Differential Resistance
R_{p1} = First Positive Differential Resistance
R_{p2} = Second Positive Differential Resistance

III. SIMULATED RESULTS AND DISCUSSIONS

A. I-V characteristic graph for Varied B1 and Fixed B2 in Thomas Fermi Model

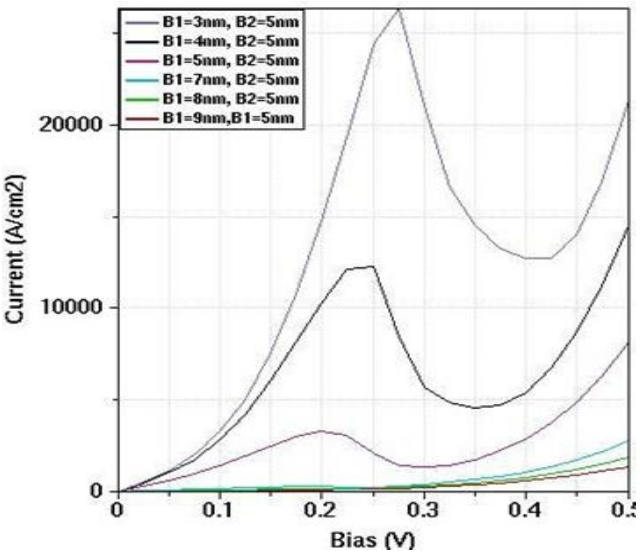

Figure 3: *Double barrier Thomas Fermi modelled RTD representing varied B1 and fixed B2.*

When the barrier width of B1 is less than B2, that is, when B1 is 3nm and 4 nm respectively and B2 is 5 nm, then peak currents are about 27000 A/cm^2 and 14000 A/cm^2 respectively at 0.27 V and 0.25 V. When both barriers are 5 nm, then peak current is approximately 3000 A/cm^2 at 0. 2V. The Peak current of symmetric barriers, i.e., B1=5 nm and B2=5 nm is about 24000 A/cm^2 less than B1=3 nm and B2=5 nm and about 11000 A/cm^2 less than B1=4 nm and B2=5 nm. In the case of the NDR region, B1=3 nm and B2=4 nm has much higher NDR compared to B1=4 nm and B2=5 nm and B1=5 nm and B2=5 nm. 0.15 V (0.42 V – 0.27V). NDR region is supplied by B1=3 nm and B2=5 nm, while 0.10V (0.35V – 0.25V) and 0.08 V (0.28V – 0.2V) NDR regions are provided by B1=4 nm and B2=5 nm and symmetric barriers of 5 nm.

The Valley current of symmetric barriers of B1=5 nm and B2=5 nm is almost 500 A/cm^2 at 0.28 V, which is 7V and 14V less than B1=4nm and B2=5nm and B1=3nm and B2=5nm respectively.

When B1 is increased than B2, i.e., when B1 is 7 nm,8 nm, and 9 nm and B2 is 5nm, then peak currents drastically reduce and create very less number of peak currents compared to the cases of B1 width larger and B2 width smaller and symmetric barriers. Such as, only about 400 A/cm^2 peak currents are provided by B1=7 nm and B2=5 nm, B1=8 nm -B2=5nm, and B1=9 nm and B2= 5 nm. Moreover, the NDR region and valley current are nearly 0 for these barriers.

To sum up, an increased width of B1 which is more than B2 is not a good approach at all, as NDR, PDR1, and PDR2 are all lost. If B1 is kept less than and equal to B2, then RTDs can be used in both digital and analog applications.

B. I-V characteristic graph for Fixed B1 and Varied B2 in Thomas Fermi Model

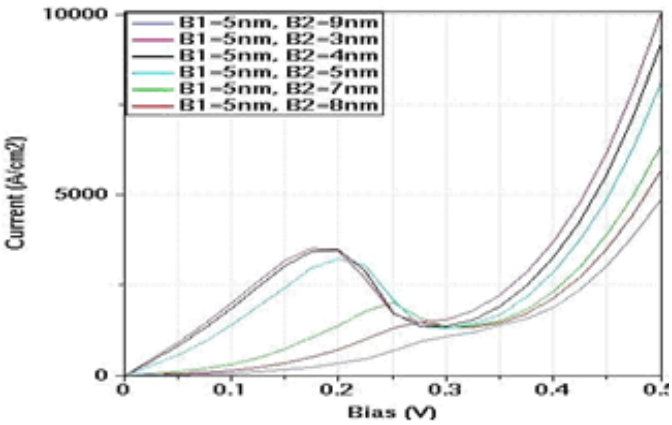

Figure 4: *Double barrier Thomas Fermi modelled RTD representing Fixed B1 and Varied B2*

When all B1 is fixed at 5 nm and B2 are varied, then peak currents, saturated currents, and valley currents are rapidly reduced compared to the case of varied B1 and fixed B2. For example, both B1=5 nm and B2=3 nm and B1=5 nm and B2=4 nm had 2700 A/cm^2 peak currents at about 0.17V. The blue wave produced a peak current at about 2600 A/cm^2 within about 0.2V.

Currents peaks produced approximately at 2300 A/cm^2, 2200 A/cm^2, and 2000 A/cm^2 by B1=5 nm and B2=7 nm, B1=5 nm and B2=8 nm, and B1=5 nm and B2=9 nm within 0.25 V, 0.26 V and 0.27V. Valley currents are 2100 A/cm^2 for B1=5 nm and B2=3 nm, B1=5nm and B2=4 nm, and B1=5 nm and B2=5nm at 0.28 V.

Valley current for the B2 and 7 nm,8 nm, and 9 nm and fixed B1 are absent. That is why NDR is not present at all.

To sum up, it can be told that B2 should always be less than and equal to B1. Otherwise, in the absence of the NDR region, RTDs would not be able to use for digital applications. They can only be used in analog applications, such as, in ultrafast pulse creation.

C. I-V characteristic graph for Varied B1 and Fixed B2 in Hartree Model

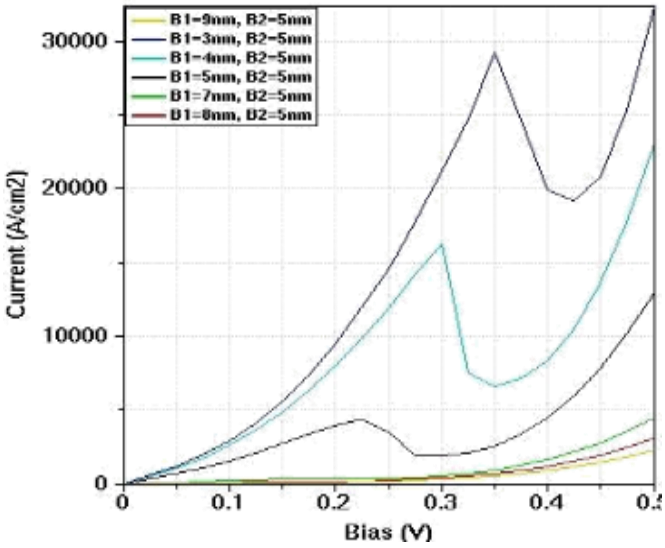

Figure 5: *Double Barrier Hartree modelled RTD representing Varied B1 and fixed B2.*

In the case of B2 fixed and B1 varying, B1 must be less than and equal to B1 if RTDs are used for a wide range of applications in both digital and analog circuits.

For the case of B1 and 7 nm,8 nm and 9 nm, and B2 and 5nm, very few currents have been supplied. No saturated current and valley current are present although about 100 A/cm^2 peak current is produced for 7 nm,8 nm, and 9 nm B2. So, no NDR region exists.

If B2=5 and nm B1=3 nm, B2=5 nm and B1=4 nm, and symmetric barriers are compared, then 5 nm B2 and 3 nm B1 has the highest peak current and 5 nm symmetric barrier of B1 and B2 5nm has the lowest peak current. 2800 A/cm^2 is

produced by 5 nm B2 and 3 nm B1, 1600 A/cm^2 is supplied by 5 nm B2 and 4 nm B1 and lastly, 4000 A/cm^2 is created by symmetric barriers at 0.35V, 0.3V, and 0.22V respectively.

Valley current of 5 nm B2 and 3 nm B1 is 17000 A/cm^2(19000A/cm^2 – 2000A/cm^2) higher than symmetric barriers and 11,500 A/cm^2(19,000A/cm^2 – 7500A/cm^2) higher than 5 nm B2 and 4 nm B1.

NDR region is 0.07 V (0.42V – 0.35V) for 3 nm B1 and 5 nm B2, 0.05V (0.35V-0.30V) for 4nm B1 and 5 nm B2 and 0.06 V (0.28V – 0.22V) for symmetric barriers. Symmetric barriers have less NDR than 3 nm B1 and 5 nm B2 and more NDR than 4 nm B1 and 5nm B2.

D. I-V characteristic graph for Fixed B1 and Varied B2 in Hartree Model

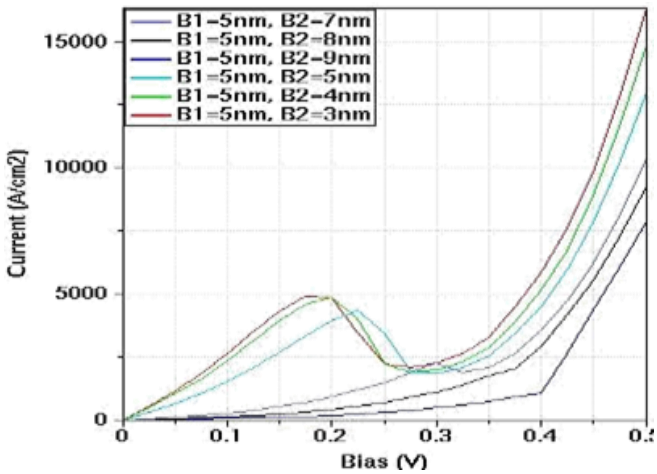

Figure 6: *Double Barrier Hartree modelled RTD representing fixed B1 and varied B2.*

B2=7 nm – B1=5 nm, B2=8 nm – B1=5 nm, and B2=9 nm – B1=5 nm supplied only 250 A/cm^2 approximately at about 0.12V. NDR regions and valley currents are almost 0. Only for these barrier widths, RTDs would act like a traditional p-n junction diode.

However, if B2 is less than and equal to B1, i.e., when B2 are 3 nm, 4 nm, and 5 nm and B1 are 5 nm, then peak and valley currents rapidly increased and much bigger and better NDR, PDR1 and PDR2 regions are produced. For example, both B1=5 nm – B2=4 nm and B1=5 nm – B2=3 nm supplied about 5000 A/cm^2 at about 0.18 V. On the other hand, symmetric barriers of B1=5 nm – B2=5 nm created about 4000 A/cm^2 at about 0.23 V, which is 1000 A/cm^2 less than B1=5 nm = B2=4 nm and B1=5 nm – B2= 3 nm. 0.05 V more voltage was needed to produce peak current in symmetric barriers than asymmetric barriers of B1=5 nm – B2=3nm and B1=5 nm – B2=4nm. Red, green, and sky-colored waves produced valley currents at almost 2400 A/cm^2 within about 0.27V.

To sum up, it can be said that B2 must not be more than B1. Otherwise, NDR, PDR1, and PDR2 regions would not be found out and RTDs would not be able to be utilized for analog and digital applications.

IV. TABLES

Table 1: *GaAs/Al0.3Ga0.7As DBRTD structure used in the simulations* [5].

Material	GaAs	GaAs	GaAs	AlGaAs	GaAs	AlGaAs	GaAs
Layer	Spacer1	Lead1	Well1	Barrier1	Spacer2	Lead2	Barrier2
Doping(/m^3)	1×10^{24}	1×10^{27}	1×10^{24}	1×10^{24}	1×10^{24}	1×10^{27}	1×10^{24}
Length (Angstrom)	100	300	50	50	100	300	50

Table 2: *Some comparisons among RTD, RTID and Esaki TD* [7].

NDR Devices	Design Flexibility	Manufacture Ability	Speed Index	Peak Voltage	Operating Principle	Carrier Transport
Esaki TD	Material and Doping Limited	Fair	Medium (less than and equal to 100)	Small	Single barrier Tunneling	Bipolar
RTD	Very Good	Good	as high as 10^3	Small to large	Resonant Tunneling	Unipolar
RITD	Material Limited	Difficult	Medium (less than and equal to 100)	Small to Large	Resonant Tunneling	Bipolar

Table 3*: Calculated Values of R_{p1}, R_n, R_{p2}, PVVR, and PVCR in the varied first barrier-fixed second barrier of a Thomas Fermi modelled DBRTD.*

Parameter	**B1(3nm) – B2(5nm)**	**B1(4nm) – B2(5nm)**	**B1(5nm) – B2(5nm)**	**B1(7nm) – B2(5nm)**	**B1(8nm) – B2(5nm)**	**B1(9nm) – B2(5nm)**
Vp (V)	0.27	0.25	0.20	0.27	0.27	0.27
I_p (A/cm^2)	27000	14000	3000	400	400	400
V_v	0.42	0.35	0.28	0	0	0
I_v	12600	4900	500	0	0	0

V_s	0.50	0.48	0.40	0	0	0
I_s	27000	14000	3000	0	0	0
R_{P1}(kilo-ohm)	$1*10^{-12}$	$1.79*10^{-12}$	$6.67*10^{-12}$	$6.75*10^{-11}$	$6.75*10^{-11}$	$6.75*10^{-11}$
R_N (kilo-ohm)	$1.04*10^{-12}$	$1.10*10^{-12}$	$3.2*10^{-12}$	$6.75*10^{-11}$	$6.75*10^{-11}$	$6.75*10^{-11}$
R_{P2}(kilo-ohm)	$5.56*10^{-13}$	$1.42*10^{-12}$	$4.8*10^{-12}$	0	0	0
PVVR	0.64	0.71	0.71	∞	∞	
PVCR	2.14	2.85	6	∞	∞	∞

Table 4*: Calculated Values of R_{p1}, R_n, R_{p2}, PVVR, and PVCR in the fixed first barrier-varied second barrier of a Thomas Fermi modelled DBRTD.*

Parameter	**B1(5nm) – B2(3nm)**	**B1(5nm) – B2(4nm)**	**B1(5nm) – B2(5nm)**	**B1(5nm) – B2(7nm)**	**B1(5nm) – B2(8nm)**	**B1(5nm) – B2(9nm)**
Vp (V)	0.17	0.17	0.20	0.25	0.26	0.27
I_p (A/cm^2)	2700	2700	2600	2300	2200	
V_v (V)	0.28	0.28	0.28	0	0	2000
I_v (A/cm^2)	2100	2100	2100	0	0	0
V_s (V)	0.39	0.39	0.40	0	0	0
I_s (A/cm^2)	2700	2700	2600	0	0	0
R_{P1} (kilo-ohm)	$6.30*10^{-12}$	$6.30*10^{-12}$	$7.70*10^{-12}$	$1.09*10^{-11}$	$1.18*10^{-11}$	$1.35*10^{-11}$
R_N (kilo-ohm)	$1.83*10^{-11}$	$1.83*10^{-11}$	$1.60*10^{-11}$	$1.09*10^{-11}$	$1.18*10^{-11}$	$1.35*10^{-11}$
R_{P2} (kilo-ohm)	$1.83*10^{-11}$	$1.83*10^{-11}$	$2.4*10^{-11}$	0	0	0
PVVR	0.60	0.60	0.71	∞	∞	∞
PVCR	1.28	1.28	1.23	∞	∞	∞

Table 5*: Calculated Values of R_{p1}, R_n, R_{p2}, PVVR, and PVCR in the varied first barrier-fixed second barrier of a Hartree modelled DBRTD.*

Parameter	**B1(3nm) – B2(5nm)**	**B1(4nm) – B2(5nm)**	**B1(5nm) – B2(5nm)**	**B1(7nm) – B2(5nm)**	**B1(8nm) – B2(5nm)**	**B1(9nm) – B2(5nm)**
Vp	0.35	0.30	0.22	0.28	0,28	0.28
I_p	28000	16000	4000	100	100	100
V_v	0.42	0.35	0.28	0	0	0
I_v	19000	7500	2000	0	0	0
V_s	0.48	0.46	0.40	0	0	0
I_s	28000	16000	4000	0	0	0
R_{P1}	$1.25*10^{-12}$	$1.88*10^{-12}$	$5.5*10^{-12}$	$2.8*10^{-10}$	$2.8*10^{-10}$	$2.8*10^{-10}$
R_N	$7.77*10^{-13}$	$5.88*10^{-13}$	$3*10^{-12}$	$2.8*10^{-10}$	$2.8*10^{-10}$	$2.8*10^{-10}$
R_{P2}	$6.67*10^{-13}$	$1.29*10^{-12}$	$6*10^{-12}$	0	0	0
PVVR	0.83	0.86	0.80	∞	∞	∞
PVCR	1.47	2.13	2	∞	∞	∞

Table 6*: Calculated Values of R_{p1}, R_n, R_{p2}, PVVR and PVCR in the fixed first barrier-varied second barrier of a Hartree modelled DBRTD.*

Parameter	**B1(5nm) – B2(3nm)**	**B1(5nm) - B2(4nm)**	**B1(5nm) – B2(5nm)**	**B1(5nm) – B2(7nm)**	**B1(5nm) - B2(8nm)**	**B1(5nm) – B2(9nm)**
Vp	0.18	0.18	0.23	0.12	0.12	0.12
I_p	5000	5000	4000	250	250	250
V_v	0.27	0.27	0.28	0	0	0
I_v	2400	2400	2400	0	0	0
V_s	0.37	0.38	0.39	0	0	0
I_s	5000	5000	4000	0	0	0
R_{p1}	$3.6*10^{-12}$	$3.6*10^{-12}$	$5.75*10^{-12}$	$4.8*10^{-11}$	$4.8*10^{-11}$	$4.8*10^{-11}$
R_n	$3.46*10^{-12}$	$3.46*10^{-12}$	$3.13*10^{-12}$	$4.8*10^{-11}$	$4.8*10^{-11}$	$4.8*10^{-11}$
R_{p2}	$3.85*10^{-12}$	$4.23*10^{-12}$	$6.88*10^{-12}$	0	0	0
PVVR	0.67	0.67	0.82	∞	∞	∞
PVCR	2.08	2.08	1.67	∞	∞	∞

V. ADVANTAGES

I. Reduced power consumption.
II. Circuit speed in a picosecond.
III. Enhanced functionality.
IV. High resistance and low capacitance to the environmental factors [6].
V. Low noise coefficient is present [6].
VI. Handling of high frequency in the terahertz range.
VII. Strongly reliable.

Longer lifespan than CMOS, MOSFET, FET, and BJT.

VI. FUTURE SCOPE

I. RTDs can be combined with Analog-to-Digital Converters (ADC) that can be used in oceanic water acoustic systems in the 2030s.
II. If a material system compatible with silicon technology is achieved, then RTDs can be used in the development of silicon-based VLSI [8].
III. RTDs perhaps can replace the robust transistors, oscillators, operational amplifiers, and frequency converters as grinders of integrated circuits within the 2030s.

VII. SUMMARY

Overall, from this vital research, it can be concluded that increasing barrier width is not a well-known approach. If RTDs have to be used in a huge variety of analog and digital applications, then the first barrier must have to be less than and equal to the second barrier, if the second barrier is kept fixed. Also, in the case of fixing the first barrier, the second barrier must be equal and less than the first barrier.

For both the models, in the case of the varied first barrier and fixed second barrier, peak current had been supplied in a higher amount than the fixed first barrier and varied second barrier when B1: 3nm,4nm, and 5nm and B2: 5nm and B1: 5nm and B2: 3nm, 4nm, and 5nm. When B1: 7 nm,8nm, and 9nm and B2: 5nm and B1: 5nm and B2: 7 nm,8nm, and 9nm in both models, the second barrier varied, and the first barrier fixed had much better and higher peak current than the case of the varied first barrier and fixed second barrier.

If models are considered, then a higher peak current is supplied by the Hartree model than Thomas Fermi model, while in Thomas Fermi model, the NDR region was created in a bigger amount compared to Hatree model.

From tables – 3,4,5 and 6, it was found that the value of PVCR is more than PVVR. In tables – 3,4,5 and 6, PVCR and PVVR are infinity for asymmetric barriers of B1: 7nm,8nm,9nm and B2=5 nm and B2: 7nm,8nm,9nm and B1=5nm. R_{p2} in all cases is 0. PVVR for table 5 is the highest and PVCR for table 3 is the highest. In tables 4 and 6, PVVR and PVCR for B1: 5 nm and B2: 3nm,4nm are the same and less than symmetric barriers. In table 5, PVVR and PVCR are higher for B1=4nm and B2=5nm than B1=3nm and B2=5nm and symmetric barriers.

VIII. CONCLUSION

RTDs have allowed understanding the particular applications that will be beyond the capability of CMOS technology [9]. These low-power, high-speed, and small devices are uniquely helpful as researchers continue to scale down to the size of atoms where heat and parasitic effects are major problems [8]. Research in Nano-electronics today stands at a frontier of semiconductor science and engineering. RTD is assumed to be a major Nanoelectronic device at the center of Nanoelectronic research.

A. Applications of RTD at Present Time:

In today's time, both single and double barrier GaAs/AlGaAs RTDs can be used in oscillators when they are implemented in negative differential resistance region and in digital logic circuits when they are implemented in bi-stable condition.:

B. Advantages of RTDs:

1. Circuit speed is enhanced.
2. Power Consumption is reduced in a great amount.
3. Functionality is increased.

C. Future Scope of RTDs:

RTDs perhaps can replace the robust transistors as the grinder of integrated circuits within 2030s.

IX. SUMMARY

After analysis of the simulated results, it can be declared that double barrier RTD is more promising than single barrier RTD, since, in the case of double barrier RTD,the current has reached at a peak value of 4800 A/cm2 at 0.25 Biased Volt, neatly the current has reached a value to almost 2400 A/cm2, which is the valley point, at 0.275 biased Volt and then has increased uup to12,500 A/cm2 at 0.5 biased Volt, whereas, in the case of single barrier RTD, the current has kept on increasing up to 10,000 A/cm2 at 0.5 biased Volt, without reaching any peak point and valley point values at specific biased voltages. It can also be seen that the model of Thomas-Fermi performs better than Hartree model considering the fact of defining NDR. Nevertheless, the Hartree model proves a better performance for applications which need higher current density in digital world. After all these inspections, it can be clearly stated that the proposed model performs more efficiently than the model described in[12].

X. CONCLUSION

Based on the simulation results we can come to the conclusion that for any applications, the Hartree model performs more accurately due to the property of having higher PVVR at positive differential resistance region in comparison to Thomas-Fermi.

REFERENCES

[1] S. Datta, "Non-Equilibrium Green's Function (NEGF) Formalism: An elementary Introduction," *Proceedings of the International Electron Devices Meeting (IEDM) - IEEE Press*, 2002.

[2] O. Pinaud, "Transient Simulations of a Resonant Tunneling Diode," *J. Appl. Phys.*, August 2002.

[3] K. H. M. T. A. M. Hasan, "Designing of GaAs based Resonant Tunneling Diode and Nano-Scale Applicayions Considering NEGF," *Journal of VLSI Design Tools and Technology (joVDTT)*, pp. 1-18, 2015.

[4] L. T. T. E. L. L. Chang, "Resonant Tunneling in Semiconductor double barriers," *Applied Physics Letters*, vol. 24, no. 12, pp. 593-595, 1974.

[5] M. R. H. Santu Saha, " Analysis of Digital Inverter using single and multiple GaAs/AlGaAs based Double Barrier Resonant Tunneling Diode," *ICIET*, p. 6, 2018.

[6] "Tunnel Diode Theory - Tunneling Effect," [Online]. Available: https://911electronic.com/tunnel-diode-theory-tunnel-effect

[7] J. P. Sang, "Resonant Tunneling Diodes: Models and Properties," May 1998. [Online].

[8] "Resonant-tunneling mixed-signal circuit technology," *Solid-State Electronics*, vol. 43, pp. 1355-1365, 1999.

[9] A. G. Akkala, " NEGF Simulation of Electron Transport in Resonant Tunneling and Resonant Interband Tunneling Diodes," Ann Arbor, 2011.

Mrs. Tahseen Asma Meem is a Lecturer at the Dept. of EEE, since 2018, Faculty of Engineering, American International University-Bangladesh (AIUB). She accomplished his B.Sc. Engg. (EEE) and M.Sc. Engg. (EEE) degree from American International University-Bangladesh, Dhaka, Bangladesh in 2015 and 2017 respectively. Mrs. Tahseen Asma Meem started her teaching career as a Teaching Assistant in Dept. of EEE and served from 11th May 2017- 17th January 2018. As a researcher, she had the opportunity to publish some research papers in reputed journals and conferences. Her paper has been published previously in IEEE explore. Apart from research experiences, she has contributed to organizing webinars and also participated in different industrial tours, workshops, webinars, and seminars. She has been an active committee member of the proofreading and documentation committee to write reports of events, webinars, and seminars held within the EEE department. Her research interests are embedded systems, Robotics, Nanotechnology, Characterization of nanoparticles, Quantum Mechanics, nanoparticles, Nano transistors, Spintronics, sensor, piezoelectric sensor, and IoT.

Shaira Tashnub Torsa is a former undergraduate student at the Department of Electrical and Electronic Engineering, Faculty of Engineering, American International University - Bangladesh from May 2017 to December 2020.She accomplished her BSc. (EEE) degree with three "Dean's List Honor" academic distinctions in 2019 and a general wavier of 25% from September 2017 to December 2020.In her undergraduate project and thesis, she designed an "Ultrasonic Blind Walking Stick" with her group which is a step towards the easy navigation of the visually challenged people on both day and night outside and inside their homes. She participated in various webinars at the University of Rajshahi and American International University – Bangladesh. She is also involved in different organizations like COURSERA, NANOHUB and nanotechnology@aiub. Her research interests are in microelectronics, nanoelectronics, nanomaterials, photovoltaics, solar cells, mid infrared emitters and receivers, medical devices, sensors and biosensors and Internet of Things.

.

Mr. Mehedi Hasan is an Assistant Professor at the Dept. of EEE, since 2018, Faculty of Engineering, American International University-Bangladesh (AIUB). He accomplished his B.Sc. Engg. (EEE) and M.Sc. Engg. (EEE) degree with the 'Summa Cum Laude' academic distinction from American International University-Bangladesh, Dhaka, Bangladesh in 2012 and 2014 respectively. Mehedi Hasan started his teaching career as a Teaching Assistant in Dept. of EEE and served from September 1, 2013, to January 13, 2015. Previously, he worked as a Lecturer for the duration of 3+ years at AIUB in his own department. As a researcher, he has published several research articles in various internationally renowned journals. He elected as a judge in different Math Olympiad, Math Quiz Contest, AIUB Jubilation, Science Congress seminars, Robotics Contest and Programming Contest. He participated various symposium, international conferences, seminars, workshops, and industrial tours in different places. He is also a Professional of IEEE USA, Member of the OBE Committee in AIUB and Committee Member of iCREST. His research interests Nanotechnology, Characterization of nano particles, Quantum Mechanics, Nanoparticle, Nano transistor, Spintronics, nano-photonics, Nano sensor, Band Structure Model, Material synthesis and characterization, green synthesis, PCF, SPR, Biosensor, solar cell, piezoelectric sensor, IoT, Deep learning(AI), VLSI & ULSI Design, Quantum wire, Quantum Dot related works.

Mahfujur Rahman received his B.Sc. in Computer Science & Engineering and M.Sc. in Intelligent Systems from American International University - Bangladesh (AIUB). After his M.Sc., he joined AIUB as a Lecturer. He has started his academic journey with AIUB and served as a Lecturer since 2020. His research interests are mainly focused on Intelligent Systems, NLP, Machine Learning, Data Science, Medical Image Processing, IoT and Big Da ta Analytics. For more than three years, he has been with the undergraduate students, as a supervisor of their thesis work. He has served as a reviewer in several local and international peer reviewed journals and conferences.

.